Available online at www.sciencedirect.com
ScienceDirect
Physica B 398 (2007) 407–411
PHYSICA B
www.elsevier.com/locate/physb

Metal-insulator transition in correlated systems: A new numerical approach

D.J. García[a], E. Miranda[a], K. Hallberg[b,*], M.J. Rozenberg[c,d]

[a]Instituto de Física Gleb Wataghin, Unicamp, CEP 13083-970 Campinas, SP, Brazil
[b]Instituto Balseiro and Centro Atómico Bariloche, CNEA, (8400) San Carlos de Bariloche, Argentina
[c]Laboratoire de Physique des Solides, CNRS-UMR8502, Université de Paris-Sud, Orsay 91405, France
[d]Departamento de Física, FCEN, Universidad de Buenos Aires, Ciudad Universitaria, Pabellón 1, Buenos Aires (1428), Argentina

Abstract

We study the Mott transition in the Hubbard model within the dynamical mean field theory approach where the density matrix renormalization group method is used to solve its self-consistent equations. The DMRG technique solves the associated impurity problem. We obtain accurate estimates of the critical values of the metal-insulator transitions. For the Hubbard model away from the particle-hole symmetric case we focus our study on the region of strong interactions and finite doping where two solutions coexist. In this region we demonstrate the capabilities of this method by obtaining the frequency-dependent optical conductivity spectra. With this algorithm, more complex models having a larger number of degrees of freedom can be considered and finite-size effects can be minimized.
© 2007 Elsevier B.V. All rights reserved.

PACS: 71.10.Fd; 71.27.+a; 71.30.+h

Keywords: Mott transition; Dynamical mean field theory; Density matrix renormalization group

1. Introduction

One of the greatest challenges nowadays is the development of reliable methods for solving problems in strongly correlated systems in which the competition between the kinetic and Coulomb energy of electrons, which are of the same order of magnitude, leads to peculiar behaviors. As analytical methods based on perturbative considerations are quite unreliable in this parameter region, it is important to consider non-perturbative techniques and numerical methods to try to deal with these difficulties.

Great theoretical progress in our understanding of the physics of strongly correlated electron systems has been possible since the introduction of the dynamical mean field theory (DMFT) [1,2]. This approach is based on the natural extension of the familiar classical mean-field theory of statistical mechanics to the treatment of models of strongly interacting electrons on a lattice. The DMFT solution of the model is exact in the limit of large lattice dimensionality or large connectivity [2,3]. It has allowed for the successful investigation of model Hamiltonians relevant to problems as diverse as colossal magnetoresistance, heavy fermions and metal-insulator transitions (MI) among others [3]. Presently, the field of realistic band structure calculations of strongly correlated systems in which density functional theory is blended with DMFT is a very active one as was recently highlighted by Kotliar and Vollhardt [4].

The key feature of DMFT is that it maps the original lattice problem onto a self-consistent quantum impurity model. This resulting quantum impurity remains, nevertheless, a fully interacting many-body problem that has to be solved [3]. Currently, many numerical techniques have been adapted to solve this quantum impurity problem as quantum Monte Carlo [5], numerical renormalization group [6,7] and exact diagonalization [8]. All these methods give complementary information but are typically limited

*Corresponding author.
E-mail address: karen@cab.cnea.gov.ar (K. Hallberg).

0921-4526/$ - see front matter © 2007 Elsevier B.V. All rights reserved.
doi:10.1016/j.physb.2007.04.049

to systems with two orbitals. A proposal was recently introduced which was based on the precise diagonalization of the quantum impurity Hamiltonian with the powerful density matrix renormalization group (DMRG) [9–11]. This method has the appealing features of making no a priori approximations, the possibility of a systematic improvement of the quality of the solutions and it is not formulated as a low-frequency asymptotic method [12]. Thus it may provide equally reliable solutions for both gapless and gapfull phases. More significantly, it provides accurate estimates for the distributions of spectral intensities of high frequency features such as the Hubbard bands, that are of main relevance for analysis of X-ray photoemission and optical conductivity experiments.

2. The method

The Hamiltonian of the Hubbard model is defined by

$$H = \frac{t}{\sqrt{2d}} \sum_{\langle i,j\rangle,\sigma} c^{\dagger}_{i,\sigma} c_{j,\sigma} + U \sum_{i} \left(n_{i,\uparrow} - \frac{1}{2}\right)\left(n_{i,\downarrow} - \frac{1}{2}\right) - \mu \sum_{i,\sigma} n_{i,\sigma}, \tag{1}$$

where U is the on-site Coulomb interaction, t is the hopping, μ is the chemical potential and d is the space dimension. We take the half bandwidth of the non-interacting model as unit of energy, thus $D = 2t = 1$. We particularize to the case of the infinite-dimensional Bethe lattice, in which the non-interacting density of states (DOS) is $D(\varepsilon) = (2/\pi)\sqrt{1-\varepsilon^2}$.

The treatment of this model Hamiltonian with DMFT leads to a mapping of the original lattice model onto an associated quantum impurity problem in a self-consistent bath. In the particular case of the Hubbard model, the associated impurity problem is the single impurity Anderson model (SIAM), where the hybridization function $\Delta(\omega)$, which in the usual SIAM is a flat density of states of the conduction electrons, is now to be determined self-consistently with the requirement that $\Delta(\omega) = t^2 G(\omega)$, where $G(\omega)$ is the impurity Green's function. At the self-consistent point $G(\omega)$ coincides with the *local* Green's function of the original lattice model [3]. A central quantity in this algorithm is the non-interacting Green's function of the impurity problem, $G_0(\omega) = 1/(\omega + \mu - \Delta(\omega)) = 1/(\omega + \mu - t^2 G(\omega))$. Since it is essentially a Green's function, $\Delta(z)$ can be decomposed into "particle" and "hole" contributions as $\Delta(z) = \Delta^{>}(z) + \Delta^{<}(z)$ with $\Delta^{>}(z) = t^2\langle gs|c(1/(z-(H-E_0)))c^{\dagger}|gs\rangle$ and $\Delta^{<}(z) = t^2\langle gs|c^{\dagger}(1/(z+(H-E_0)))c|gs\rangle$ for a given Hamiltonian H with ground-state energy E_0. By standard Lanczos technique, H can be tri-diagonalized and the functions $\Delta^{>}(z)$ and $\Delta^{<}(z)$ can be expressed in terms of respective continued fractions [13]. As first implemented in Refs. [8,14], each continued fraction can be represented by a chainof auxiliary atomic sites whose energies and hopping amplitudes are given by the continued fraction diagonal and off-diagonal coefficients, respectively. From the self-consistency condition, the two chains representing the hybridization, are "attached" to the right and left of an atomic site to obtain a new SIAM Hamiltonian, H_{SIAM}. In fact $G_0(z)$ constitutes the local Green's function of the site plus chain system.

The algorithm in Refs. [8,14], basically consists in switching on the local Coulomb interaction at the impurity site of the SIAM Hamiltonian and use the Lanczos technique to re-obtain $\Delta(z)$, iterating the procedure until the set of continued fractions coefficients converges.

Diagonalizing the Hamiltonian using DMRG, allows to handle chains of arbitrary length [15]. Here we used up to 101 sites keeping 128 states per block.

The SIAM Hamiltonian reads

$$H_{\mathrm{SIAM}} = \sum_{\substack{\sigma,\alpha=-N_C \\ \alpha\neq 0}}^{N_C} a_\alpha c^{\dagger}_{\alpha\sigma} c_{\alpha\sigma} + \sum_{\substack{\sigma,\alpha=-(N_C-1) \\ \alpha\neq 0,-1}}^{N_C-1} b_\alpha (c^{\dagger}_{\alpha\sigma} c_{\alpha+1\sigma} + \mathrm{h.c.}) + \sum_{\sigma,\alpha=\pm 1} b_0 (c^{\dagger}_{\sigma} c_{\alpha\sigma} + \mathrm{h.c.}) + U\left(n_\uparrow - \frac{1}{2}\right)\left(n_\downarrow - \frac{1}{2}\right) - \mu(n_\uparrow + n_\downarrow) \tag{2}$$

with c_σ being the destruction operator at the impurity site, and $c_{\alpha\sigma}$ being the destruction operator at the α site of the hybridization chain of $2N_C$ sites. The set of parameters $\{a_\alpha, b_\alpha\}$ are directly obtained from the coefficients of the continued fraction representations of $\Delta(z)$ by the procedure just described.

3. Results

3.1. Half-filled Hubbard model

In Fig. 1 we show the DMFT + DMRG results (solid lines) for the DOS for several values of increasing interaction U. The results are compared to the iterated perturbation theory (IPT) results (dashed lines) [1,16] which is a useful analytic approximate method that can be solved on the real frequency axis at $T = 0$. It can be seen that for U/D not too close to the coexistence region IPT gives results which are consistent with DMRG.

At large values of the interaction the system evolves toward an insulating state with a gap of order U. It was seen [9] that a metallic state only exists if the self-consistent equations are solved in chains larger than a critical length L_c. In Fig. 2 we present results of the divergence of L_c and also show the closure of the gap as a function of U. A distinctive feature of the metal-insulator transition in the paramagnetic state of the Hubbard model at half-filling [3] is that there are two distinct critical values of the interaction associated with the transition: U_{c1} and U_{c2}. The former signals the insulator to metal transition obtained upon lowering the interaction, while the latter corresponds to the metal-to-insulator transition obtained when the Fermi liquid is destroyed by increasing the

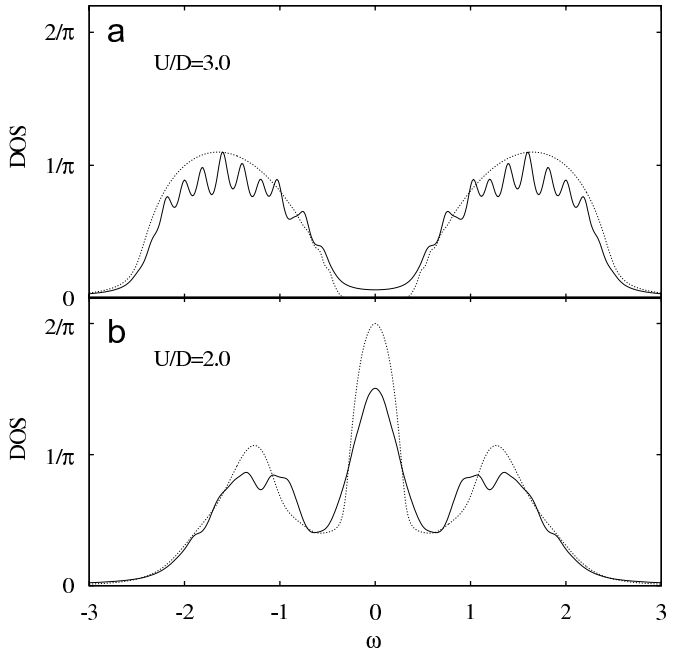

Fig. 1. Density of states $\mathrm{DOS} = (1/\pi)\,\mathrm{Im}\,G(\omega + 0.1I)$ corresponding to the half-filled Hubbard model (solid lines). We also show the IPT results (dashed lines).

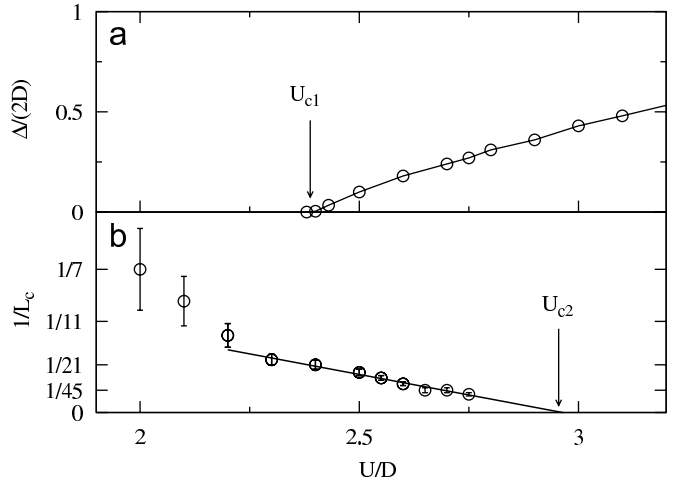

Fig. 2. (a) Extrapolated gap (circles) and (b) critical length L_c as a function of interaction U (for large U/D symbols are larger than the error bars).

interaction strength and is signaled by the divergence of L_c. We obtained estimates of these two values that are consistent with those from NRG calculations [6]. We find $U_{c1} = 2.39 \pm 0.02$ and $U_{c2} = 2.95 \pm 0.05$. Our criterion for the investigation of metallic versus insulating states was based on the behavior of L_c and the size of the gap in the DOS (given by the energy of the first pole).

3.2. Doped Hubbard model

In this section we illustrate the application of this new method to the Hubbard model away from particle-hole symmetry, focusing on the region of the phase diagram where two solutions coexist near the correlation-driven Mott metal-insulator transition and obtain the phase boundaries with unprecedented precision [17]. We also illustrate the capabilities of the methodology by computing the frequency-dependent optical conductivity, which requires the reliable description of higher energy features, such as the Hubbard bands, that lie beyond the scope of the NRG method.

In Fig. 3 we show the evolution of the DOS for the two solutions as one moves away from the half-filled particle-hole symmetric case. The chemical potential μ is increased at fixed U. The results show that, in the insulating case, when the chemical potential is moved within the Mott gap, the lower and upper Hubbard bands shift rigidly, without any ostensible transfer of spectral weight taking place (Fig. 3(a)). The apparent substructure in the Hubbard bands seen in the insulating DOS results from finite-size effects. In contrast, in the lightly doped case one observes that, as the central quasi-particle peak rapidly moves through the region between the Hubbard bands, there is a transfer of spectral weight as well as an evolution of the line shapes (Fig. 3(b)). More precisely, one finds that the quasi-particle peak receives spectral weight from both

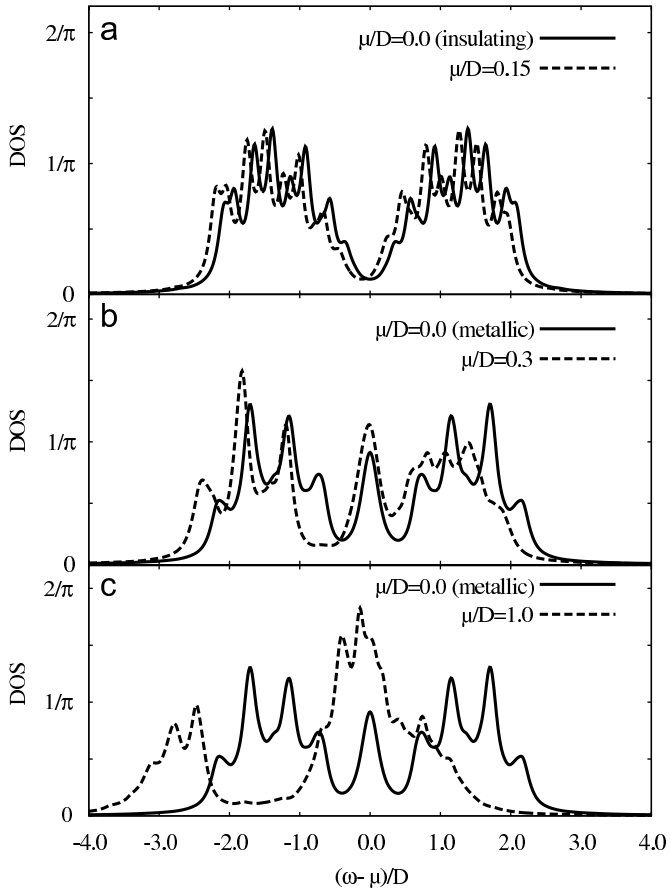

Fig. 3. Density of states (DOS) for the Hubbard model ($U/D = 2.6$) at three different dopings: (a) insulating, (b) lightly doped and (c) heavily doped metallic cases. The finite DOS in (a) at the Fermi energy is due to the broadening used.

Hubbard bands. For larger values of μ, as the system gets heavily doped, one finds that the quasi-particle peak eventually broadens as it merges with the closest Hubbard band (Fig. 3(c)). As these features coalesce, they also draw spectral weight from the other Hubbard band that remains at an energy distance of the order of U [3].

We have also computed the frequency-dependent optical conductivity. From the lattice Green's $G(\varepsilon_k, \nu)$ function, where ε_k is the non-interaction dispersion, we can evaluate the optical conductivity within DMFT as [3,18]:

$$Re\,\sigma(\omega + I0^+) = \frac{\pi e^2}{\hbar a d} \int_{\infty}^{\infty} d\varepsilon\, D(\varepsilon) \int_{\infty}^{\infty} d\nu \times \rho(\varepsilon, \nu)\rho(\varepsilon, \nu + \omega) \frac{\theta(\nu + \omega) - \theta(\nu)}{\omega}, \quad (3)$$

where a is the lattice spacing, d is the spatial dimension, $\rho(\varepsilon, \nu) = \mathrm{Im}\, G(\varepsilon, \nu - I0^+)/\pi$, and $I0^+$ denotes an infinitesimal imaginary part. The evaluation of $\rho(\varepsilon, \nu)$ requires the previous computation of the local self-energy. While in the standard exact diagonalization solution of the DMFT equations this is a cumbersome procedure due to the small number of Green's function poles, the use of DMRG dramatically changes the situation and reliable $\Sigma(\omega)$ on the real axis can be easily obtained from the self-consistency condition [3]. In Fig. 4 we show the optical conductivity for two coexistent solutions (for parameters $U/D = 2.6$ and $\mu = 0.2$) and for the metallic state for weak interaction ($U/D = 0.6$). In the metallic case we see that, despite the very small doping, the small frequency regime of $\sigma(\omega)$ can be very well described by a simple Lorentzian form that follows from a Drude model [19]:

$$Re\,\sigma(\omega + I0^+) = \frac{DW\tau}{1 + (\omega\tau)^2}, \quad (4)$$

where τ is the relaxation time and DW is the Drude weight, which is a measure of the number of quasi-particle carriers in the metal. For large U/D we observe that, in addition to the small Drude part, the optical conductivity spectrum has a large mid-infrared contribution at frequencies of order U. This regular part corresponds to finite frequency optical excitations between the two Hubbard bands and between the latter and the central quasi-particle peak and is almost absent for small values of the Coulomb interaction.

In Fig. 5(a) we show the evolution of the doping for fixed chemical potential, varying the Coulomb interaction. The doping increases as μ moves to larger values, i.e., away from the particle-hole case. At fixed μ, increasing the correlation U from the non-interacting limit acts to decrease δ continuously to 0, where the metallic solution is no longer stable and gives rise to the insulating one. The extrapolation of the lowest doping values towards zero for different chemical potentials provides an accurate estimate of the critical line $\mu_{c2}(U)$ which locates the instability of the metal towards an insulating solution. The DW is shown in Fig. 5(b). Its behavior is qualitatively different from that of δ, since $DW(U)$ does not uniformly increase with increasing μ. In the low U/D region, the DW decreases as the chemical potential is increased, reflecting the lowering of the kinetic energy due to the fewer number of carriers. In contrast, for larger values of the interaction close to the μ_{c2} line, the DW decreases as μ decreases towards particle-hole symmetry, reflecting the enhancement of the effective mass as the metal-insulator transition is approached.

We have also investigated the instability of the insulating state towards the metal. This transition is signaled by the collapse of the Mott–Hubbard gap as the chemical potential is brought to a Hubbard band edge. Following the energy of the lowest unoccupied state (LUS) in the upper Hubbard band with respect to the Fermi level in the insulator as μ increases, it is possible to determine the transition line $\mu_{c1}(U)$ (Fig. 5(c)) as the value of the critical chemical potential for which the energy of the LUS vanishes. As the bands move in an approximately rigid way for $\mu < \mu_{c1}(U)$ the value of the chemical potential varies linearly and agrees with half the size of the band gap at $\mu = 0$ (see Fig. 6). For $\mu > \mu_{c1}(U)$ a finite number of

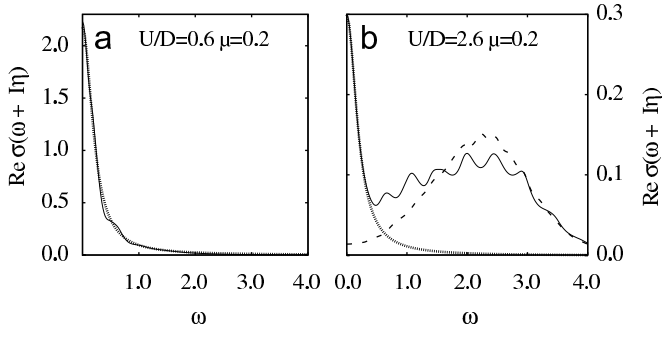

Fig. 4. Metallic (solid line) and insulating (dashed) optical conductivities for the Hubbard model in the purely metallic (a) and coexistent (b) regimes. The dotted line is a Lorentzian low-frequency fit (Drude model). For small U/D, the data and the Lorentzian fit agree in almost all the frequency ranges.

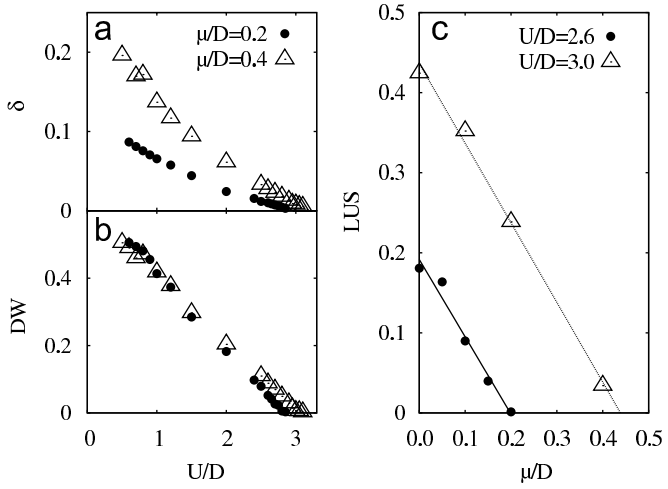

Fig. 5. (a) Doping δ and (b) Drude weight (DW) for the metallic states for various U/D and μ/D values. (c) Energy of the lowest unoccupied state (LUS) in the upper Hubbard band for insulating solutions.

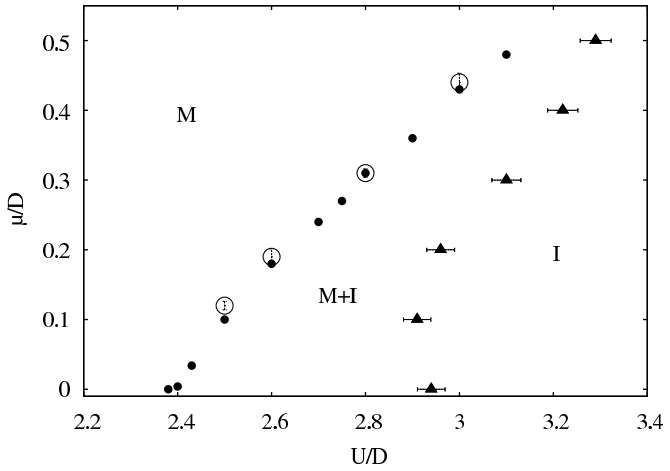

Fig. 6. Phase diagram: small full circles show half the gap value for $\mu = 0$. Empty circles (full triangles) are the extrapolated critical values of the chemical potential μ_{c1} (μ_{c2}) where the insulating (metallic) solution no longer exists.

poles appear at positive and negative small values of $\omega - \mu$, signaling the metallic state.

In Fig. 6 we present results for the critical lines which draw the phase diagram of the model away from particle-hole symmetry at $T = 0$. We plot the $\mu_{c1}(U)$ and $\mu_{c2}(U)$ lines that determine three regions in the μ-U phase diagram: for $\mu > \mu_{c1}(U)$ ($\mu < \mu_{c2}(U)$) only metallic (insulating) solutions are found. In the middle there is a region of coexistence of both kinds of states. The phase diagram presented here shows an overall agreement with the one obtained through exact diagonalization in the "star geometry" [20] where the impurity site is connected with hopping terms to all the other sites. The main differences are found for the $\mu_{c2}(U)$ line because, as the metal to insulator transition is approached, the quasi-particles develop a diverging mass corresponding to a very narrow quasi-particle peak. In the language of the associated SIAM, this narrow resonance implies a large correlation length which can be fully realized only in long enough systems. This can only be obtained with the method presented here, allowing for very accurate results.

4. Conclusions

We have shown that the DMRG method, in addition to being largely used to compute spectral quantities of low-dimensional strongly correlated systems allows for a practical implementation of an accurate impurity solver of the DMFT equations of the Hubbard model in a general case. We have computed the density of states and the frequency-dependent optical conductivity as well as the behavior of the doping and the Drude weight as a function of the chemical potential near the metal-insulator transition. We have demonstrated the accuracy of the method by making a comparison of the respective predictions of these quantities for the metal-insulator critical line. Due to the fact that with this method long enough systems can be handled, these critical lines can be very accurately obtained.

The implementation of the DMRG method within the DMFT is an important step towards achieving an exact, unbiased and general impurity solver to be used in a realistic *ab initio* strongly correlated electronic structure calculation program [4]. The next step ahead is to generalize the methodology for the multi-orbital case, where interesting physical problems remain open, such as the orbital-selective Mott transition with a fully rotationally invariant Hamiltonian.

DJG acknowledges support form the FAPESP. EM acknowledges support from FAPESP and CNPq. We also acknowledge support from CONICET, the Guggenheim Foundation, the ECOS-Secyt programme and PICT 03-06343 and 03-13829 of ANPCyT.

References

[1] A. Georges, G. Kotliar, Phys. Rev. B 45 (1992) 6479.
[2] W. Metzner, D. Vollhardt, Phys. Rev. Lett. 62 (1989) 324.
[3] A. Georges, G. Kotliar, W. Krauth, M.J. Rozenberg, et al., Rev. Mod. Phys. 68 (1996) 13.
[4] G. Kotliar, D. Vollhardt, Phys. Today 53 (2004).
[5] G. Kotliar, S. Murthy, M.J. Rozenberg, Phys. Rev. Lett. 89 (2002) 046401.
[6] R. Bulla, Phys. Rev. Lett. 83 (1999) 136.
[7] R. Bulla, T. Costi, D. Vollhardt, Phys. Rev. B 64 (2001) 045103.
[8] Q. Si, et al., Phys. Rev. Lett. 72 (1994) 2761.
[9] D.J. García, K. Hallberg, M.J. Rozenberg, Phys. Rev. Lett. 93 (2004) 246403.
[10] S. Nishimoto, F. Gebhard, E. Jeckelmann, J. Phys.: Condens. Matter 16 (2004) 7063–7081;
F. Gebhard, et al., Eur. Phys. J. B 36 (2003) 491.
[11] M. Karski, C. Raas, S. Uhrig, Phys. Rev. B 72 (2005) 113110.
[12] C. Raas, G. Uhrig, F.B. Anders, Phys. Rev. B 69 (2004) 041102(R).
[13] K. Hallberg, Phys. Rev. B 52 (1995) 9827.
[14] M.J. Rozenberg, G. Moeller, G. Kotliar, Mod. Phys. Lett. B 8 (1994) 535.
[15] I. Peschel, X. Wang, M. Kaulke, K. Hallberg (Eds.), Density Matrix Renormalization, Lectures Notes in Physics, Springer, Berlin, 1999;
S.R. White, Phys. Rev. Lett. 69 (1992) 2863.
[16] X.Y. Zhang, M.J. Rozenberg, G. Kotliar, Phys. Rev. Lett. 70 (1993) 1666;
X.Y. Zhang, M.J. Rozenberg, G. Kotliar, Phys. Rev. B 48 (1993) 7167;
A. Georges, W. Krauth, Phys. Rev. B 48 (1993) 7167–7182.
[17] D. García, E. Miranda, K. Hallberg, M. Rozenberg, Phys. Rev. B 75 (2007) 121102(R).
[18] M.J. Rozenberg, G. Kotliar, H. Kajueter, G.A. Thomas, D.H. Rapkine, J.M. Honig, P. Metcalf, Phys. Rev. Lett. 75 (1995) 105.
[19] J.M. Ziman, Principles of the Theory of Solids, second ed., 1986, p. 280.
[20] H. Kajueter, G. Kotliar, Phys. Rev. Lett. 77 (1996) 131–134;
H. Kajueter, G. Kotliar, G. Moeller, Phys. Rev. B 53 (1996) 16214.